

# Study of MPP Techniques for Photovoltaic Systems

Haneesh Babu Karalikkattil Thanduparakkal<sup>1</sup>, Dharmaian Retnam Binu Ben Jose<sup>2</sup>

<sup>1,2</sup>Vellore Institute of Technology Chennai, Tamil Nadu, India

**Abstract**— This work presents an extensive study of maximum power point tracking (MPPT) techniques using three algorithms when photovoltaic (PV) array is subjected to USC (uniform shaded condition) and partial shaded condition (PSC). MPPT techniques including incremental conductance (IC), fuzzy logic control (FLC), and hill-climbing (HC), techniques are the most intentional customary techniques. For discovering the maximum power point (MPP) of the PV module under every concealing condition, the above MPPT techniques are concomitantly using deviations of the PV current and voltage. Each algorithm proves to provide certain advantages to make it applied widely. The disadvantages however do not hinder the applicability. Hence, a comparison of the performance of traditional MPPT algorithms such as HC, IC, and FLC methods has been carried out in this article. A simple boost converter with a resistive load modeled using MATLAB/Simulink has been applied for the experimentation of several MPPT algorithms. For PV researchers to remain updated with the most recent progress, it is visualized that this study will be a source of significant data.

**Index Terms**—Solar energy, Photovoltaic (PV), Partial shading, Maximum power point, Uniform shading.

## I. INTRODUCTION

Solar energy is regarded as the main promising and probably to be the basis of a sustainable energy economy among renewable sources. Because of the economic prospects of medium and long-term PV power systems in large capacity are being installed worldwide [1]. Configurations like series, parallel, and series-parallel (SP) are typically used [2].

Because of the non-linearity in the output voltage ( $V_{PV}$ ) as well as current ( $I_{PV}$ ) of the PV array, there is one MPP in the P–V (power-voltage) characteristics under USC [3]. Hence, the MPPT technique is typically introduced for maximizing the PV power [4]. The extraction of maximum power is done by placing a power conditioning unit that is interfaced between PV modules and the load. The other function of this conditioning unit is to ensure the control of the output current and voltage-independent variations in load and input voltage [5].

Because of the clouds and shadows of adjacent buildings and trees, some portions of the PV exhibit get meagre sun-powered illumination. Hence, incomplete shading in PV systems cannot be avoided [6]. The system P–V characteristic curve has many peaks during the partial shaded condition (PSC) or in mismatching condition [7 – 9].

## II. PV CELL MODELING

A simple PV framework of PV array is shaped by connecting a large number of PV modules either in series or parallel or series-parallel mode through a centralized inverter as illustrated in Figure 1. For ensuring the required current and voltage, the PV cluster comprises many PV modules associated in series & parallel mode [10]. With each PV module to be protected from the hot-spot issue, bypass diodes are coupled in parallel. The jamming diode is associated in arrangement with each string to defend the modules from the impact potential difference among series-linked strings which is grouped in series-parallel PV modules [11].

The mathematical expression of the output current for each module is

$$I = I_{pc} - I_{01} \left[ \exp \left( \frac{V_{pv} + I_{pv} R_s}{a_1 V_{T1}} \right) - 1 \right] - I_{02} \left[ \exp \left( \frac{V_{pv} + I_{pv} R_s}{a_2 V_{T2}} \right) - 1 \right] - \left( \frac{V_{pv} + I_{pv} R_s}{R_p} \right) \quad (1)$$

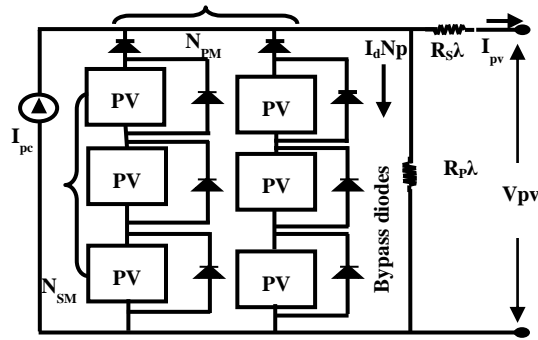


Figure 1. Series – Parallel combination of PV module

where  $I_{pv}$  &  $V_{pv}$  indicate PV current and voltage respectively,  $I_{pc}$  indicates the light-produced current by the PV cell,  $I_{01}$  &  $I_{02}$  signifies the diode reverse saturation currents as per two PV cell diode model.  $I_{02}$  compensates for the recombination loss in the diode's depletion region (1), The thermal voltage of the PV module is

$$V_{T1,2} = N_s kT/q \quad (2)$$

where  $N_s$  represents the number of series-connected cells,  $q$  indicates the electron charge ( $1.602 \times 10^{-19}C$ ),  $k$  signifies the Boltzmann constant ( $1.3806503 \times 10^{-23} J/K$ ) and  $T$  denotes the temperature of the PN junction in K. The terms  $a_1$  &  $a_2$  are the ideality constants of the diode [12]. In the two diode model, the accuracy is high. But, seven parameters are to be evaluated namely  $I_{pc}$ ,  $I_{01}$ ,  $I_{02}$ ,  $R_p$ ,  $R_s$ ,  $a_1$ , and  $a_2$ . The values  $a_1$  and  $a_2$  has been assumed as  $a_1 = 1$  and  $a_2 = 2$ . The output equation is then,

$$I = I_{pc} - I_0 \left[ \exp\left(\frac{V_{pv} + I_{pv}R_s}{V_T}\right) + \exp\left(\frac{V_{pv} + I_{pv}R_s}{(p-1)V_T}\right) - 2 \right] - \left(\frac{V_{pv} + I_{pv}R_s}{R_p}\right) \quad (3)$$

$$I_{pc} = (I_{SC\_STC} + K_i \Delta T) \frac{G}{G_{STC}} \quad (4)$$

Where  $I_{SC\_STC}$  indicates the photo generated current at STC (standard test condition) in Ampere. From (4)

$$\Delta T = T - T_{STC} \text{ K } (T_{STC} = 25^{\circ}C)$$

$G$  indicates the actual irradiation of the cell along with  $G_{STC}$  ( $1000 \text{ W/m}^2$ ) is the irradiation at STC and  $K_i$  denotes the current coefficient of the short circuit. The saturation current may be calculated as,

$$I_{01} = I_{02} = I_0 \quad (5)$$

$$I_0 = \frac{(I_{SC\_STC} + K_i \Delta T)}{\exp\left[\frac{(V_{OC\_STC} + K_v \Delta T)}{\{(1+a_2)/p\} V_T}\right] - 1} \quad (6)$$

$$p = 1 + a_2 \geq 2.2 \quad (7)$$

where,  $V_{oc,STC}$  is the PV cell voltage on the open circuit at STC,  $K_v$  is a constant. The iteration technique is used to calculate the parameters  $R_s$  and  $R_p$  in (1). The output equation of the model in Figure 1; is,

$$I = N_{PM} \left\{ I_{pc} - I_0 \left[ \exp\left(\frac{V_{pv} + I_{pv}R_s \lambda}{V_T N_{SM}}\right) + \exp\left(\frac{V_{pv} + I_{pv}R_s \lambda}{(P-1) V_T N_{SM}}\right) - 2 \right] \right\} \quad (8) \text{ Then, the } \lambda \text{ value is written as}$$

$$- \left(\frac{V_{pv} + I_{pv}R_s \lambda}{R_p \lambda}\right) \quad (9)$$

$$\lambda = \frac{N_{SM}}{N_{PM}}$$

where  $N_{SM}$  and  $N_{PM}$  are represented as the quantity of PV array modules associated with SP.

For building an array preliminary from the elemental cell to the main assembly, it offers a hypothetical bit-by-bit strategy. On the ideal PV cell interconnections, the aim is to learn the authority of various weather conditions for the cell quality and the categories of module technologies, and the dependence of cell interconnection is also projected [13].

### A. PARTIAL SHADED CONDITION ON PV ARRAY

Non-uniform operating conditions are caused by several factors such as aging, partial shading, and dust. When partial shading takes place, the shaded panels will act as a load instead of a generator where hot spots are produced and finally destroys the panel [14 - 17]. The photocurrent for the shaded PV cells decreases, though the un-shaded cells maintain a higher photocurrent as the short-circuit current of a PV cell is relative to the irradiation level. Which causes a fall in the effective output current and hence the output power. This effect is termed as partial shading effect [18]. The pictorial representation of partial shading is illustrated in Figure 2. A portion of the PV modules, which receive uniform irradiation, will work with the most extreme efficiency [19].

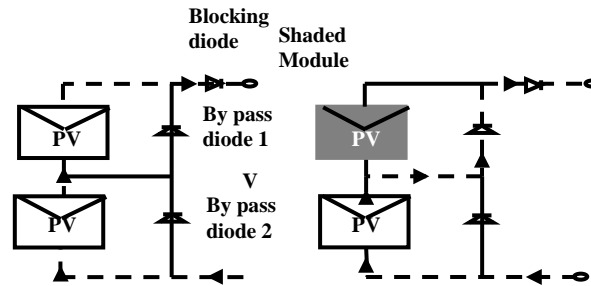


Figure 2. PV array under normal operation and partial shaded condition

The P-V and I-V characteristics demonstrating the PSC under different shading conditions are displayed in Figure 3. Two conceivable cases are portrayed (a) with bypass diode and (b) without bypass diode. The diodes are used to divert the PV current from a shaded module. Therefore, the heating and array losses are decreased [20]. The execution of the bypass diode is shown in Figure 2 and the expression is,

$$PV_2 - \sum_{i=1}^n PV_i \geq V_D \quad i \neq 2 \quad (10)$$

From (10), it is comprehended that MPPT techniques are crucial for following the worldwide pinnacle viably under PSC; as multiple peaks happen under this condition [21]. Subsequently, the MPPT technique ought to have the capacity to find this global peak effectively.

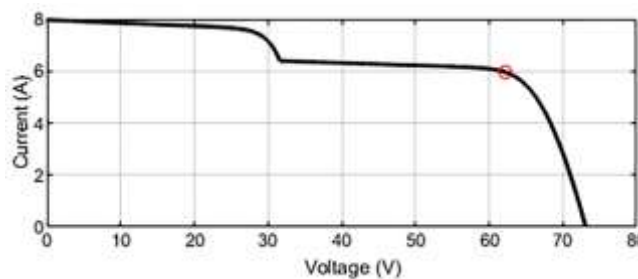
The principle of MPPT may be described with the help of Figure 4. At MPP ( $V_{mpp}$ ,  $I_{mpp}$ ), the PV module produces its most extreme output power ( $P_{mpp}$ ) as follows:

$$P_{mpp} = V_{mpp} \times I_{mpp} \quad (11) \quad \text{where } I_{mpp} \text{ and } V_{mpp} \text{ indicate the ideal MPP current as well as the voltage of the PV module respectively.}$$

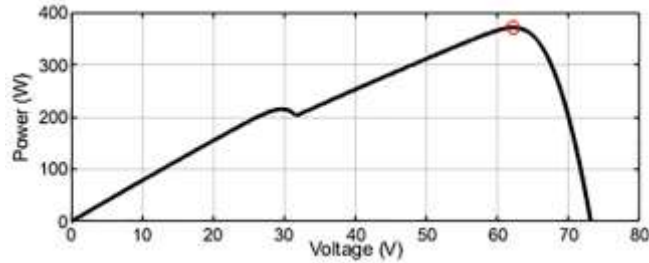
At the point when a PV module is associated with a load, the working purpose of the PV module should be at the convergence of its I-V curve and the load line. A resistive load has a 1/R slope with a straight load line. A power electronic controller is introduced in the solar PV cluster and the load to extract extreme power. This converter adjusts load power to the array power so that the load characteristic is changed along the locus of MPP and maximum power is transferred from the array. The D (duty cycle) of this converter is modified until it gets the MPP [22].

The primary objectives of the MPPT controller are:

- 1) To reduce the output power fluctuations in the steady-state
- 2) To lessen the framework control misfortune
- 3) To achieve the MPP with a small-time increase in the transitional state of the process
- 4) Stability
- 5) Robustness



(a)



(b)

Figure 3. PV array Performance under the partial shaded condition with respect to (a) I-V characteristic (b) P-V characteristic

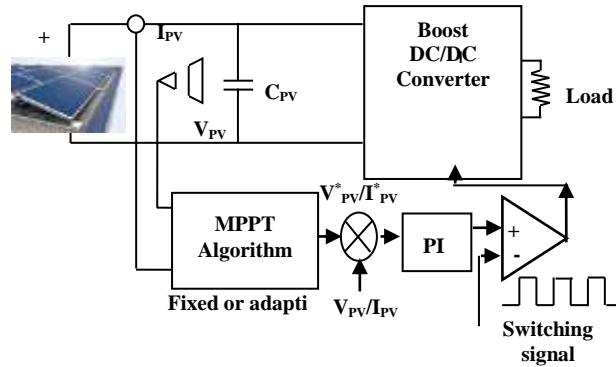


Figure 4. Block diagram of PV array with MPPT techniques

### III. TYPES OF MPP TECHNIQUES

The two conventional MPPT techniques named IC and HC and an advanced technique named fuzzy logic controller (FLC) are analysed here.

#### A. INCREMENTAL CONDUCTANCE METHOD (IC)

In incremental conductance technique, the slope of the power characteristic (Figure 3) in the PV cluster is specified by,

$$\left. \begin{aligned} \text{At MPP} &\Rightarrow dP_{pv}/dV_{pv} = 0 \\ \text{In the left of MPP} &\Rightarrow dP_{pv}/dV_{pv} > 0 \\ \text{In the right of MPP} &\Rightarrow dP_{pv}/dV_{pv} < 0 \end{aligned} \right\} (12)$$

$$\text{As, } \frac{dP_{pv}}{dV_{pv}} = \frac{d(IV)_{pv}}{dV_{pv}} = I + V \frac{dI_{pv}}{dV_{pv}} \cong I + V \frac{\Delta I}{\Delta V} \quad (13)$$

Then (12) can be rephrased as,

$$\left. \begin{aligned} \text{At MPP} &\Rightarrow \Delta I/\Delta V = -I/V \\ \text{In the left of MPP} &\Rightarrow \Delta I/\Delta V > -I/V \\ \text{In the right of MPP} &\Rightarrow \Delta I/\Delta V < -I/V \end{aligned} \right\} (14)$$

Thus, the MPP would be pursued by associating the “instantaneous conductance” ( $I/V$ ) to the “incremental conductance” ( $\Delta I/\Delta V$ ). The  $V_{ref}$  (“reference voltage”) is the MPP voltage at which the PV cluster is required to operate. At the MPP,  $V_{MPP}$  would be equivalent to  $V_{ref}$ . At the point when the MPP is attained, the PV operating point would be preserved until a change in  $\Delta I$  is recorded. The algorithm alters the  $V_{ref}$  in order to trail the value of the new MPP [23 - 25]. The key principle of the IC technique is an incremental comparison of instantaneous conductance with the ratio of conductance derivative [26].

The increment step size regulates how quickly the MPP is obtained. Tracking speed may be increased with higher increments in the step size. Though, the plan probably won't work absolutely at the MPP and swing about it rather; so there is a tradeoff. A technique has been projected that brings the working point of the PV cluster near the MPP in a primary phase and afterward uses IC to precisely follow the MPP in a secondary phase [27]. The linear performance is utilized to partition the I-V plane into two arenas, one comprising of all the conceivable MPPs under varying irradiation. A small value of error is to be added so as to reduce the oscillations between MPP which determines the sensitivity of the system and is articulated as,

$$e = \frac{I}{V} + \frac{dI_{pv}}{dV_{pv}} \quad (15)$$

### B. HILL CLIMBING METHOD (HC)

HC algorithm is fundamentally similar to perturb & observe (P & O). It adjusts the voltage of the PV array to trail the finest point  $V_{MPP}$ . The duty ratio of the boost converter in the HC algorithm is perturbed to detect the MPP. The finest point is constantly traced and validated using the algorithm until the MPP, well-characterized as  $(dP_{PV}/dV_{PV} = 0)$  is identified. The present estimation of the PV power  $P(k)$  is continually associated with the previously identified power  $P(k-1)$ . At the point when these quantities are comparable, the regulator will perturb the PV voltage and PV current once again. To bring the error  $e$  to zero, a simple proportional-integral (PI) control is incorporated.

However, when the current power is better than the past, the inclination of the power is enhanced [28]. The power converter's duty ratio remains to change and the operating power of the MPP oscillates.

The HC algorithm is described by the mathematical equation as given in (12). The key benefit of the HC algorithm is its simple operation. The disadvantage of the technique is that it fails to trace the MPP under quickly varying conservational circumstances. A modified adaptive hill climbing MPPT method has been introduced, where the parameters are automatically tuned and control the scheme. This algorithm can be implemented under numerous environmental changes [29 - 30].

### C. FUZZY LOGIC CONTROL (FLC)

FLC system with polar data is defined for the MPPT control of the PV scheme under shaded conditions. The advantages of FLC over the customary regulators are:

(i) they don't require a precise numerical model, (ii) they can work with vague information sources, (iii) they can knob non-linearity and (iv) they are more forceful than predictable non-linear controllers.

The procedure of FLC is related to simplicity and efficacy for both linear and non-linear schemes. FLC has three significant phases, fuzzification, fuzzy rule base as well as defuzzification [31 - 32]. The procedure of the FLC is revealed in Figure 5.

Fuzzification: In fuzzification, the numerical variable is rehabilitated into a linguistic variable. Seven fuzzy levels like PB (positive big), NB (negative big), PM (positive medium), NM (negative medium), PS (positive small), Z (zero) and NS (negative small), were utilized for high accuracy.

In Table 1; the Z (zero) corner to corner connotes the exchanging line which isolates the tables into two segments of control activities. Over the exchanging line, it gives a negative sign to deceleration control activity and beneath the exchanging line gives positive signs for increasing speed control activity [33].

Membership function: The controller inputs (Error:  $E$ , change of error:  $\Delta E$ ) and incremental change within the "controller output" ( $\Delta U$ ) are well-characterized on the collective normalized range of (0, 1). The membership functions are measured and their depiction is demonstrated in Figure 6. The  $dP_{PV}/dV_{PV}$  vanishes at the MPP utilizes the approximation,

$$E(m) = \frac{P(m) - P(m-1)}{V(m) - V(m-1)} \quad (16)$$

$\Delta E(m) = E(m) - E(m-1)$  (17) where,  $m$  indicates the sampling time,  $P(m)$  denotes the immediate power of the PV scheme and  $V(m)$  provides the conforming sudden voltage [34]. The  $E(m)$  will display the location of the MPP. The parameter  $\Delta E(m)$  specifies the direction of movement of the operating point.

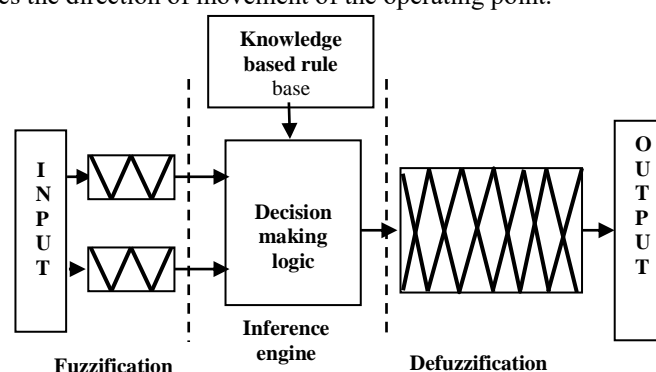


Figure 5. Fuzzy logic controller block diagram

Fuzzy rule base: The rule base that acquaints the fuzzy yield to the fuzzy data is derivative by understanding scheme behavior. The fuzzy standards are intended to integrate the accompanying consultations considering the overall following presentations.

1. When the terminal voltage of the PV cluster is larger than the MPP voltage, at that point increment in duty ratio ( $D$ ) of the converter for maintaining the terminal voltage to  $V_{mp}$ .

2. When the cluster voltage is extremely near MPP voltage and is up and coming quickly, the adjustment in duty ratio ought to be zero to deflect working point deviation away from the MPP and protect at zero change.

3. When the cluster voltage is near  $V_{mp}$ , the variation in duty ratio is little.
4. When the terminal voltage of the PV cluster is less than MPP voltage, the change in duty ratio is negative to carry the terminal voltage to  $V_{mp}$ .

TABLE 1. FUZZY RULE

$\Delta d$	$\Delta P$						
$\Delta I$	NB	NM	NS	Z	PS	PM	PB
NB	Z	NS	NS	NM	NM	NB	NB
NM	PS	Z	NS	NM	NM	NM	NB
NS	PS	PS	Z	NS	NS	NM	NM
Z	PM	PS	PS	Z	NS	NS	NM
PS	PM	PM	PS	PS	Z	NS	NS
PM	PB	PM	PM	PS	PS	Z	NS

These standards can be occupied with any PV scheme for MPP nevertheless of size and sort of converter utilized. There are various potential blends of the level of assistance with fluctuating qualities to the closely resembling standards, to content unique conditions.

Defuzzification: The FLC yield regulator is rehabilitated back to mathematical factors from etymological factors with the help of similar participation execution however with dissimilar extents relying upon customer differentiation. The yield of the FLC would give an output signal to handling the duty ratio of the power converter so as to trace the highest power yield. Due to defuzzification, the FLC will achieve a maximum working voltage under PS alignments by maintaining the PV arraignment to its maximum value. Henceforth, the energy conversion efficacy of the scheme can be enhanced [35 - 36]. On the basis of the research, if the PV cluster has encountered 50 % of concealing, the working voltage is capable to move where power is ideal related to the ordinary P&O that trap on any local peaks. Here, the information, yield etymological factors are dictated by five levels as appeared in Table 1 [37].

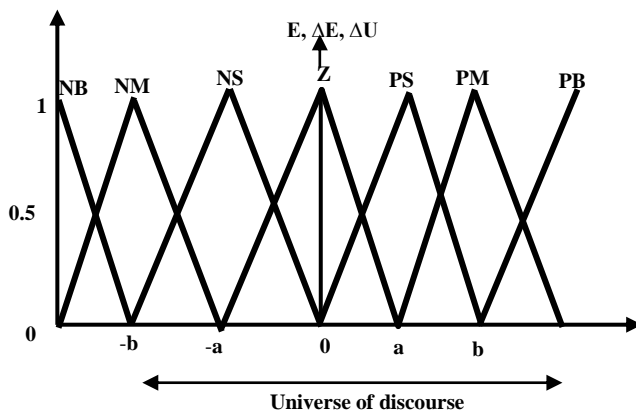


Figure 6. The fuzzy logic controller membership function

#### IV. DC TO DC CONVERTER

There are several DC to DC converters used for standalone or grid-linked PV systems to control the load. Two types of converter applied for PV systems are used at static and dynamic irradiation conditions [54]. The converter used here for enhancing the PV module performance acts as an interface among PV modules as well as load. A simple boost converter has been utilized to boost the voltage that is received from the photovoltaic module. According to the PV module rating, a fixed resistive load is used here. The duty ratio of the boost converter is derived by

$$D = 1 - (V_o / V_s) \tag{18}$$

where  $V_s$  indicates the supply voltage and  $V_o$  is the output voltage.

The voltage output of the boost converter is based on the values of duty ratio 'D'. The converter is operated in current mode continuously.

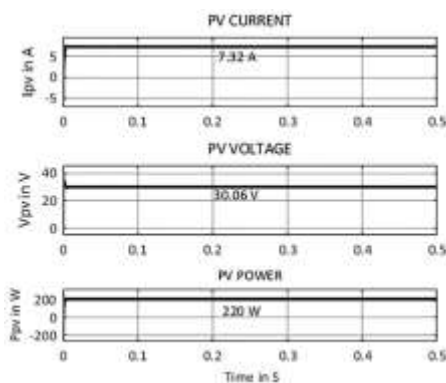
#### V. SIMULATION RESULTS

The MPPT techniques discussed in section 2 have been compared and verified using the MATLAB/Simulink model of simple boost configuration. Using the equations in section 2, a complete PV arrangement was designed as well as simulated in MATLAB/Simulink by taking the values of the components as  $C_S = 50 \mu F$ ,  $L = 100 \text{ mH}$ ,  $C_L = 50 \mu F$ . One PV module has been used for simulation of the system in USC having specifications as open-circuit voltage = 36.72 V, maximum power rating = 219.978 W, and short circuit current = 7.98 A. Two PV panels of the same rating mentioned above were connected in series for analyzing the results of PSC.

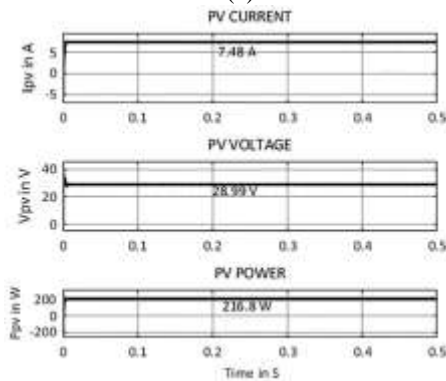
Figure 7(a); shows the steady-state PV current, voltage, and power under open-loop conditions. On analysis, it is found that in all three cases the deviation of power is approximately the same and the tracking has been carried out at the same power. When the duty ratio is at 0.35, the maximum power has been attained in the open-loop MPPT control. Various parameters such as IPV, VPV, and PPV with irradiation  $G = 1000 \text{ w/m}^2$  and  $T$  of  $25^0 \text{ C}$  in case of HC method, IC method, and FLC method are demonstrated in Figure 7(b), 8(a), & 8(b). In an open-loop arrangement, it is determined that the maximum power is 220 W under standard test conditions. It is clear that in HC method, it provides an excellent tracking ability by delivering power of 216.8 W. In the IC method, the maximum power is improved than HC and is equal to 218.3 W.

Figure 8(b); shows the steady-state result of PV system under  $G = 1000 \text{ W/m}^2$  and  $T = 25^0 \text{ C}$  for FLC based MPPT tracking. Here, the maximum power has been exactly tracked, and the value is found to be 219.9 W. The simulations for HC, IC, and FLC MPPT methods were carried out under uniform shading by changing the solar irradiation from  $1000 \text{ W/m}^2$  to  $500 \text{ W/m}^2$  as well as back to  $1000 \text{ W/m}^2$ , and the outcomes are demonstrated in Figure 9(a), 9(b) and 12(a) respectively. The irradiation was reduced after a particular time interval (at 0.1s, the irradiation has been decreased from  $1000 \text{ W/m}^2$  to  $500 \text{ W/m}^2$ ) and again brought to the same irradiation after a particular time interval (at 0.3s, the irradiation has been raised from  $500 \text{ W/m}^2$  to  $1000 \text{ W/m}^2$ ).

The outcome of various PV parameters of HC under USC is revealed in Figure 9(a), and it is clear that initially, the maximum power is at 216.8 W up to 0.2 s at irradiation of  $1000 \text{ W/m}^2$ . At 0.2 s, the irradiation is reduced to  $500 \text{ W/m}^2$  from  $1000 \text{ W/m}^2$  and it is reported that the maximum power is 59.5 W. The results of different parameters of the IC MPPT method are shown in Figure 9(b). It is understood that the initial value of maximum power is at 218.3 W up to 0.2 s at irradiation of  $1000 \text{ W/m}^2$ . At 0.2 s, the irradiation is reduced to  $500 \text{ W/m}^2$  from  $1000 \text{ W/m}^2$  and it is noticed that the maximum power is 60.8 W. The outcomes of the PV system applying the FLC MPPT technique demonstrated in Figure 12(a) clearly show that the value of maximum power initially is 219.9 W up to 0.2 s at irradiation of  $1000 \text{ W/m}^2$ . When the irradiation is reduced to  $500 \text{ W/m}^2$  from  $1000 \text{ W/m}^2$ , the maximum power has been found to be 64 W.

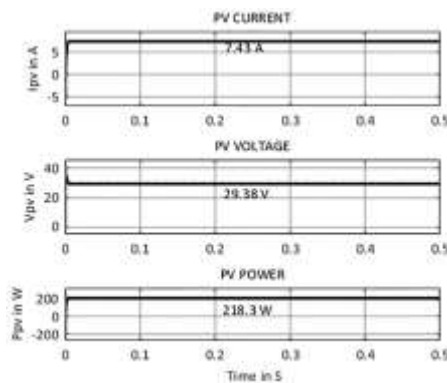


(a)

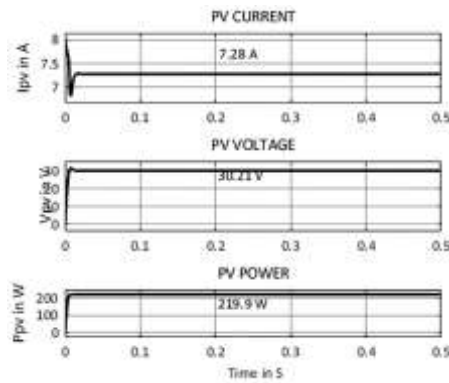


(b)

Figure 7. PV current, voltage, and power for (a) open loop system (b) HC at  $25^0 \text{ C}$  and  $1000 \text{ W/m}^2$



(a)



(b)

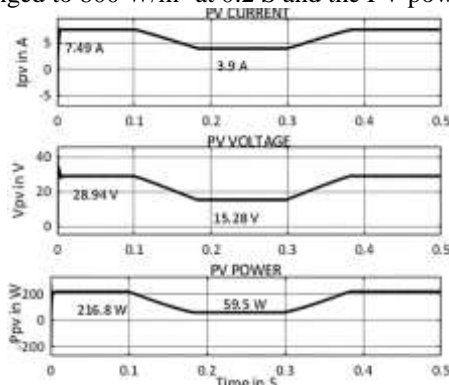
Figure 8. PV current, voltage and power for (a) IC (b) FLC at 25<sup>0</sup> C and 1000 W/m<sup>2</sup>

The steady-state power ripples for various MPPT techniques under USC are shown in Figure 10(a). It is observed that the least ripple has been found in the FLC method whereas the highest ripple was in the HC method. It was found in all methods of MPPT, the tracking of power for particular irradiation has been approximately the same.

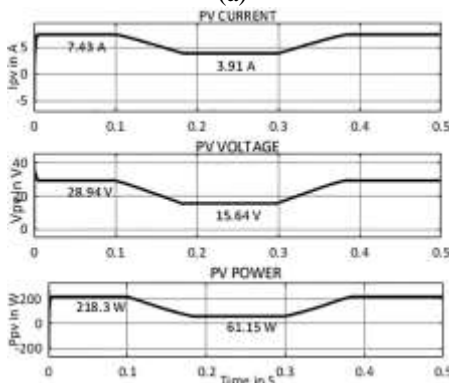
However, the tracking speed of HC is small compared with the IC method and the fastest tracking was found in FLC as demonstrated in Figure 10(b). Table 2 summarizes the simulation results for several MPPT methods for different irradiances and a temperature of 25<sup>0</sup> C. It is obvious from the table that the fuzzy logic control technique of MPPT provides better results both in the speed of tracking and accuracy. Table 2 is plotted with irradiation on X-axis as well as power on Y-axis which is shown in Figure 11(a). It is obvious that the fuzzy logic control MPPT is the best method out of the other two methods. Figure 11(b) demonstrates the comparison of maximum power error with respect to irradiation.

From Figure 11(b) it is understood that the HC technique has the highest error in power when compared with the IC and FLC and the least error in power is in FLC. Table 3 explains the comparative analysis of the three MPPT techniques in terms of tracking time, power ripple, implementation, and accuracy. It is clear that the FLC approach is better compared to the other methods presented in this paper.

Figure 12 (b) demonstrates the simulation output of the FLC under PSC. For analyzing this condition, two identical panels (each of capacity 220 W) were investigated, and initially, the irradiation for both panels is given as 1000 W/m<sup>2</sup> and the PV power is 439.7 W. The irradiation of one panel is changed to 800 W/m<sup>2</sup> at 0.2 S and the PV power at that time is 316.97 W.

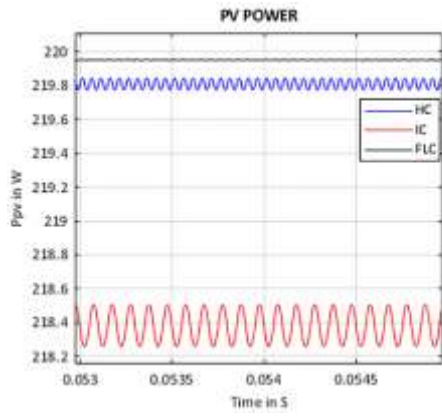


(a)

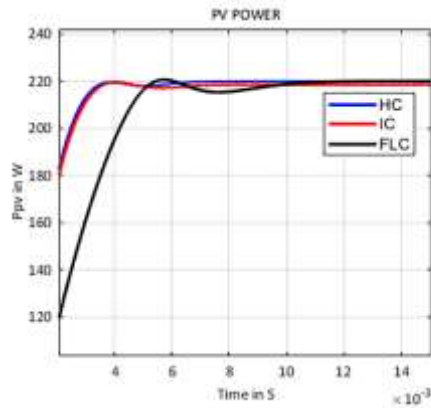


(b)

Figure 9. PV current, voltage, and power for (a) HC (b) IC under the USC

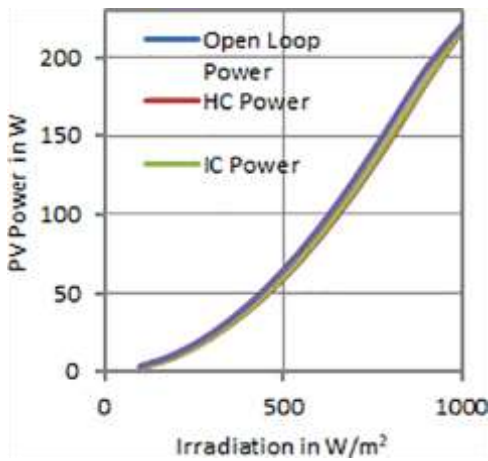


(a)

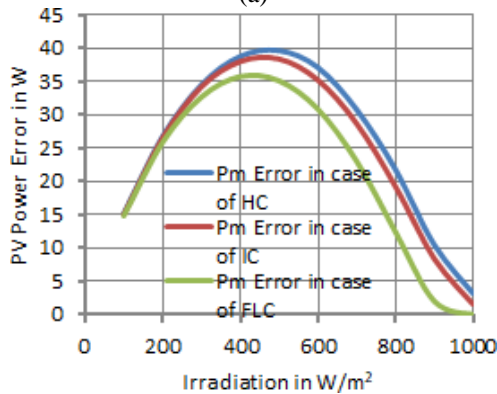


(b)

Figure 10. (a) Error in power (b) PV power tracking speed in case of HC, IC, and FLC under USC



(a)



(b)

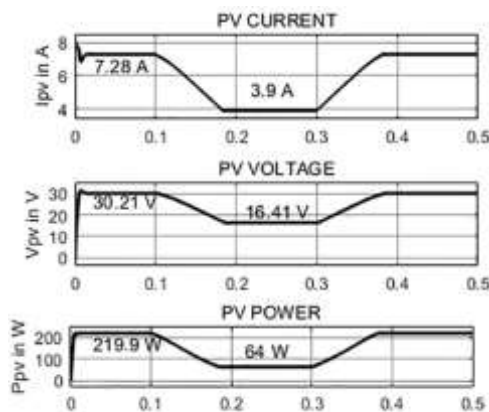
Figure 11. (a) Comparison of PV power versus irradiation for OL, HC, IC, and FLC (b) Error in Power with calculated values for different MPP techniques.

TABLE II COMPARISON OF POWERS FOR DIFFERENT MPPT METHODS

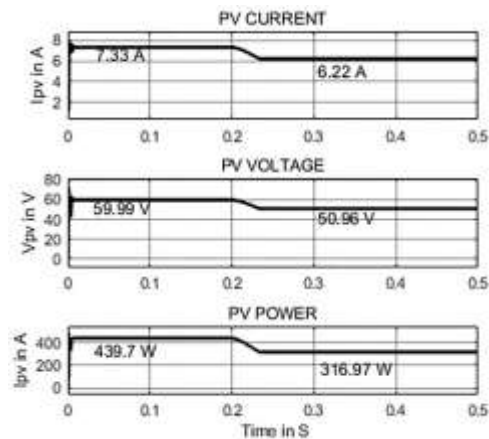
Irradiation in W/m <sup>2</sup>	Power in W			
	Open Loop	HC	IC	FLC
1000	220.00	216.80	218.30	219.90
900	192.40	183.70	185.70	192.10
800	156.80	147.40	149.90	156.70
700	122.00	114.20	116.30	121.90
600	90.90	84.60	86.50	90.80
500	64.02	59.50	60.80	64.00
400	41.70	38.70	39.50	41.70
300	24.03	22.20	22.50	23.98
200	11.04	10.20	10.40	11.00

TABLE III COMPARISON OF DIFFERENT MPPT ALGORITHMS

Scheme of MPPT	Tracking Time, S	Power ripple, %	Complexity	Accuracy	PV array Dependency
HC	6 x e-3 -- Fast	0.07	Simple	Low	No
IC	6.5 x e-3 -- Fast	0.25	Complex	Medium	No
FLC	9 x e-3 -- Fast	0.01	Complex	High	Yes



(a)



(b)

Figure 12. PV current, voltage and power for FLC under (a) USC (b) PSC

## VI. CONCLUSION

The HC, IC, and FLC methods were simulated in the MATLAB/Simulink platform. The simulation was carried out using a boost converter in open-loop as well as closed-loop with HC, IC, and FLC algorithms. It is found that all methods may be used for better tracking of maximum power. It is observed that the FLC approach is faster converging to maximum power with lesser ripples. The performance of all the three MPPT algorithms was simulated, compared, and is summarized in Table 3. The comparison shows that the FLC approach is better for tracking the maximum power and takes only very little time for settling. The PSC in the PV array creates more complex P-V characteristics with many peaks which may lead the PV cluster to trap the local MPP and diminish the maximum generation. In the case of partial concealing, the FLC method provides a better tracking ability among the methods considered in this paper.

## REFERENCES:

- [1] Jubaer Ahmed, Zainal Salam, "A Maximum Power Point Tracking (MPPT) for PV system using Cuckoo Search with partial shading capability", *Applied Energy*, Vol. 119, pp. 118-130, (2014). DOI: 10.1016/j.apenergy.2013.12.062.
- [2] Eftichios, Koutroulis, Frede, Blaabjerg, "A New Technique for Tracking the Global Maximum Power Point of PV Arrays Operating Under Partial-Shading Conditions", *IEEE Journal of Photovoltaics*, Vol.2, no.2, pp.184-190, (2012). DOI: 10.1109/JPHOTOV.2012.2183578.
- [3] Mohammadmehdi, Seyedmahmoudian, Rasoul, Rahmani, Saad, Mekhilef, Amanullah, Maung Than Oo, Alex, Stojcevski, Tey, Kok, Soon, Alireza, Safdari, Ghandhari, "Simulation and Hardware Implementation of New Maximum Power Point Tracking Technique for Partially Shaded PV System Using Hybrid DEPSO Method", *IEEE Transactions on Sustainable Energy*, Vol. 6, no. 3, pp. 850 - 862, (2015). DOI: 10.1109/TSTE.2015.2413359.
- [4] Abou, soufyane Benyoucef, Aissa, Chouder, Kamel, Kara, Santiago Silvestre and Oussama Ait sahed, "Artificial bee colony based algorithm for maximum power point tracking (MPPT) for PV systems operating under partial shaded conditions", *Applied Soft Computing*, Vol. 32, pp. 38-48, (2015). DOI: 10.1016/j.asoc.2015.03.047.
- [5] Tsang, K, M, and Chan, W, L, "Maximum power point tracking for PV systems under partial shading conditions using current sweeping", *Energy Conversion and Management*, Vol. 93, pp. 249-258, (2015). DOI: 10.1016/j.enconman.2015.01.029.
- [6] Yi-Hua, Liu, Chun-Liang, Liu, Jia-Wei, Huang and Jing-Hsiau, Chen, "Neural-network based maximum power point tracking methods for photovoltaic systems operating under fast changing environments", *Solar Energy*, Vol. 89, pp. 43-53, (2013). DOI: 10.1016/j.solener.2012.11.017.
- [7] Ahmed, K, Abdelsalam, Ahmed, M, Massoud, Shehab, Ahmed and Prasad, N, Enjeti, High-Performance Adaptive Perturb and Observe MPPT Technique for Photovoltaic-Based Micro grids", *IEEE transactions on power electronics*, Vol. 26, no. 4, pp. 1010-1021, (2011). DOI: 10.1109/TPEL.2011.2106221.
- [8] Sheik Mohammed, S, Devaraj, D, and Imthias, Ahamed, T, P, "Modeling, Simulation and Analysis of Photovoltaic Modules under Partially Shaded Conditions", *Indian Journal of Science and Technology*, Vol. 6, no. 19, pp. 1-9, (2016). DOI: 10.17485/ijst/2016/v9i16/92751.
- [9] Ishaque, K and Salam, Z, "A Deterministic Particle Swarm Optimization Maximum Power Point Tracker for Photovoltaic System Under Partial Shading Condition", *IEEE Transactions on Industrial Electronics*, Vol. 60, no. 8, pp. 3195-3206, (2013). DOI: 10.1109/TIE.2012.2200223.
- [10] Malathy, S and Ramaprabha, R, "Comprehensive analysis on the role of array size and configuration on energy yield of photovoltaic systems under shaded conditions", *Renewable and Sustainable Energy Reviews*, Vol. 49, pp. 672-679, (2015). DOI: 10.1016/j.rser.2015.04.165.
- [11] Young-Hyok, Ji, Doo-Yong, Jung, Jun-Gu, Kim, Jae, -Hyung Kim, Tae-Won, Lee and Chung-Yuen, Won, "A Real Maximum Power Point Tracking Method for Mismatching Compensation in PV Array Under Partially Shaded Conditions" *IEEE Transactions on Power Electronics*, Vol. 2, no. 4, pp. 1001-1009, (2011). DOI: 10.1109/TPEL.2010.2089537.

- [12] Makbul, A.M, Ramli, Kashif, Ishaque, Faizan, Jawaid, Yusuf, A. Al-Turki, Zainal, Salam, "A modified differential evolution based maximum power point tracker for photovoltaic system under partial shading condition", *Energy and Buildings*, Vol. 103, pp. 175-184, (2015). DOI: 10.1016/j.enbuild.2015.06.058.
- [13] Yi-Hua, Liu, Jing-Hsiao, Chen, Jia-Wei, Huang, "A review of maximum power point tracking techniques for use in partially shaded conditions", *Renewable and Sustainable Energy Reviews*, Vol. 41, pp. 436-453, (2015). DOI: 10.1016/j.rser.2014.08.038.
- [14] Srinivasa Roa, P, Saravana Ilango. G, Chilakapati Nagamani "Maximum power from PV arrays using a fixed configuration under different shading conditions," *IEEE Journal of Photovoltaics*, Vol. 4, no. 2, pp. 679-686, (2014). DOI: 10.1109/JPHOTOV.2014.2300239.
- [15] Indu Rani, B, Saravana Ilango, G, Chilakapati Nagamani "Enhanced power generation from PV array under partial shading conditions by shade dispersion using SU DO Ku configuration," *IEEE Transactions on Sustainable Energy*, Vol. 4, no. 3), pp. 594-601, (2013). DOI: 10.1109/TSTE.2012.2230033.
- [16] Indu Rani. B, Saravana Ilango. G, Chilakapati Nagamani "Impact of partial shading on the output power of PV systems under partial shading conditions," *IET Power Electronics*, Vol.7, no. 3, pp. 657-666, (2014). DOI: 10.1049/iet-pel.2013.0143.
- [17] Ali, Bidram, Ali, Davoudi, Robert, S, Balog, "Control and Circuit Techniques to Mitigate Partial Shading Effects in Photovoltaic Arrays", *IEEE Journal of Photovoltaic*, Vol. 2, no. 4, pp. 532-546, (2012). DOI: 10.1109/JPHOTOV.2012.2202879.
- [18] Basim A. Alsayid, Samer Yassin Alsadi, Jafar Jallad, Muhammad H. Dradi, "Partial Shading of PV System Simulation with Experimental Results," *Smart Grid and Renewable Energy*, Vol. 4, no. 6, pp. 429-435, (2013). DOI: 10.4236/sgre.2013.46049.
- [19] Leopoldo Gil-Antonio, Martha Belem Saldivar-Marquez, Otniel Portillo-Rodriguez, Maximum power point tracking techniques in photovoltaic systems: A brief review, in *IEEE 13th International Conference on Power Electronics (CIEP)*, © CIEP (2016). DOI: 10.1109/CIEP.2016.7530777.
- [20] Jubaer Ahmed Zainal Salam, "An improved perturb and observe (P&O) maximum power point tracking (MPPT) algorithm for higher efficiency", *Applied Energy*, Vol. 150, pp. 97-108, (2015). DOI: 10.1016/j.apenergy.2015.04.006.
- [21] Ali Nasr Allah Ali, Mohamed H. Saied, M. Z. Mostafa, T. M. Abdel- Moneim, "A survey of maximum PPT techniques of PV systems," *2012 IEEE Energytech*, Cleveland, OH, pp. 1-17, (2012). DOI: 10.1109/EnergyTech.2012.6304652.
- [22] T. Boutabba, S. Drid, L. Chrifi-Alaoui, M. Ouriagli; M.E.H. Benbouzid, "dSPACE Real-Time Implementation of Maximum Power Point Tracking Based on Ripple Correlation Control (RCC) Structure for Photovoltaic System", In *Proceeding IEEE conference on system and control*, pp. 371-376, (2016). DOI: 10.1109/ICoSC.2016.7507066.
- [23] Boualem Bendib, Hocine Belmili, Fateh Krim, "A survey of the most used MPPT methods: Conventional and advanced algorithms applied for photovoltaic systems", *Renewable and Sustainable Energy Reviews*, Vol. 45, pp. 637-648, (2015). DOI: 10.1016/j.rser.2015.02.009.
- [24] Eid A. Gouda, Mohamed. F. Kotb, and Dina A. Elalfy, "Modelling and Performance Analysis for a PV System Based MPPT Using Advanced Techniques", *EJECE, European Journal of Electrical and Computer Engineering* Vol. 1. No. 3, (January 2019). DOI: 10.24018/ejece.2019.3.1.47.
- [25] Ratnakar Babu Bollipo, Suresh Mikkili1, Praveen Kumar Bonthagorla, "Critical Review on PV MPPT Techniques: Classical, Intelligent and Optimisation", *IET Renewable Power Generation*, Vol. 14 no. 9, pp. 1433 – 1452, (2020). DOI: 10.1049/iet-rpg.2019.1163.
- [26] Trishan Eram, Patrick L. Chapman, "Comparison of Photovoltaic Array Maximum Power Point Tracking Techniques", *IEEE Transactions on Energy Conversion*, Vol. 22, no. 2, pp. 439-449, (2007). DOI: 10.1109/TEC.2006.874230.
- [27] Mojtaba Heydari; Keyue Smedley, "Comparison of maximum power point tracking methods For medium to high power wind energy systems," In *proceeding IEEE Conference on Electrical Power Distribution Networks*, pp. 184-189, (2015). DOI: 10.1109/EPDC.2015.7330493.
- [28] Saad Motahhir, Aboubakr El Hammoumi, Abdelaziz El Ghzizal, "The Most Used MPPT Algorithms: Review and the Suitable Low-cost Embedded Board for Each Algorithm", *Journal of Cleaner production*, Vol. 246, (2020). DOI: 10.1016/j.jclepro.2019.118983.
- [29] Azem H Mostafa, Amir M Ibrahim, Wajid R Anis, "A performance analysis of a hybrid golden section search methodology and nature- inspired algorithm for MPPT in a solar PV system", *Archives of Electrical Engineering*, Vol. 68, no. 3, pp. 611-627, (2019). DOI: 10.24425/ae.2019.129345.
- [30] Abdelaziz Talha, Houria Boumaaraf and Omar Bouhali, "Evaluation of maximum power point tracking method for photovoltaic system", *Archives of Control Sciences*, Vol. 21, no. 2, pp. 151-165, (2011). DOI: 10.2478/v10170-010-0037-0.
- [31] Mummadi Veerachary, Tomonobu Senjyu, Katsumi Uezato, "Neural-Network-Based Maximum-Power-Point Tracking of Coupled-Inductor Interleaved-Boost-Converter-Supplied PV System Using Fuzzy Controller", *IEEE Transactions on Industrial Electronics*, Vol. 50, no. 4, pp. 749-759, (2003). DOI: 10.1109/TIE.2003.814762.
- [32] Syafaruddin, Karatepe, E, Hiyama, T, "Artificial neural network-polar coordinated fuzzy controller based maximum power point tracking control under partially shaded conditions", *IET Renewable Power Generation*, Vol. 3, no. 2, pp. 239-253, (2009). DOI: 10.1049/iet-rpg:20080065.
- [33] Muhammad Ammirul Atiqi Mohd Zainuri, Mohd Amran Mohd Radzi, Azura Che Soh, Nasrudin Abd Rahim, "Development of adaptive perturb and observe-fuzzy control maximum power point tracking for photovoltaic boost dc-dc converter", *IET Renewable Power Generation*, Vol. 8, no. 2, pp. 183-194, (2014). DOI: 10.1049/iet-rpg.2012.0362.

- [34] Rasoul, Rahmani, Mohammadmehdi, Seyedmahmoudian, Saad Mekhilef, Rubiyah Yusof", Implementation Of Fuzzy Logic Maximum Power Point Tracking Controller For Photovoltaic System ", American Journal of Applied Sciences, Vol. 10, no. 3, pp. 209-218, (2013). DOI: 10.3844/ajassp.2013.209.218.
- [35] Abderrahman Seddjar, Kamel Djamel Eddine Kerrouche, Lina Wang, "Simulation of the proposed combined Fuzzy logic control for MPPT and Battery charge regulation used in Cubesat", Archives of Electrical Engineering, Vol. 69, no. 3, pp. 521-543, (2020). DOI: 10.24425/aee.2020.133916.
- [36] C H Hussain Basha and C Rani "Different Conventional and Soft Computing MPPT Techniques for Solar PV Systems with High Step-up Boost Converters: A Comprehensive analysis", Energies Vol. 13, pp. 371, (2020). DOI: 10.3390/en13020371.
- [37] Hiren Patel; Vivek Agarwal, MATLAB-Based Modeling to Study the Effects of Partial Shading on PV Array Characteristics, IEEE Transactions on Energy Conversion, Vol. 23, no. 1, pp. 302-310, (2008). DOI: 10.1109/TEC.2007.914308.